Roll-to-roll Imprinted Plasmonic Structural Colors

E. Højlund-Nielsen*, T. Mäkelä**, J. Clausen***, L. Thamdrup****, M. Zalkovskij****, T. Nielsen****, J. Ahopelto**, N. A. Mortensen***, A. Kristensen*

* Technical University of Denmark, DTU Nanotech, Ørsteds Plads, DK-2800 Kgs. Lyngby, Denmark
** VTT Microsystems and Nanoelectronics, P.O. Box 1000, FI-02044 VTT, Finland
*** Technical University of Denmark, DTU Fotonik, Ørsteds Plads, DK-2800 Kgs. Lyngby, Denmark
**** NIL Technology ApS, Diplomvej 381, DK-2800 Kgs. Lyngby, Denmark

ABSTRACT

Plasmon color technology based on aluminum has recently been firmly established as a route towards structural coloring of polymeric materials. We report on the fabrication of colors by localized surface plasmon resonances (LSPR) using roll-to-roll printing and demonstrate a route for scalable production and commercial uptake of plasmonic colors.

Keywords: plasmonics, surface plasmons, color, nanolithography, roll-to-roll printing

1 INTRODUCTION

Today colorants, such as pigments or dyes, are used to color plastic-based consumer products, either as base for solid colored bulk polymer or in inks for surface decoration. After usage, the products must be mechanically sorted by color before recycling [1], limiting any large-scale efficient recycling effort. As an alternative to chemistry-based coloring, nano-scale structural coloring has been proposed [2] to reduce the number of materials needed and to increase pattern resolution. Here colors are created by structural based light-matter interactions in the surface. Thereby, the sorting by color can be avoided in the recycling state, as destruction of the nano-scale texture removes any color perception leaving a (semi)-transparent bulk polymer ready for reprocessing. Nano-scale structural coloring provides new perspectives for recycling and sustainability of plastic products.

Recently, plasmon color technology based on aluminum has been firmly established as a route towards structural coloring of polymeric materials [3, 4]. Aluminum has been shown to be superior to typical plasmonic materials, such as silver [5] and gold [6], due to its natural abundance, low cost, protective oxide layer for high durability [7, 8, 9] and attractive plasmonic properties in the visible range [10, 11, 12, 13, 14, 15, 16, 17]. Based on aluminum, reflective plasmonic colors utilizing the concept of localized surface plasmon resonances (LSPR) have been presented [3, 4, 18, 19]. Here, the hybridization between LSPR modes [20] in aluminum nanodisks and nanoholes has been used to design and fabricate bright angle-insensitive colors tunable across the visible spectrum. Finally, the structural color effects can be made robust for everyday use by applying a protective coating on top, which leads to a red-shift of the plasmonic resonances [3].

Due to these considerable advances, the research and development targets are now shifting from proof-of-concept based on LSPR modes in aluminum towards increasing the color gamut and introduce scalable fabrication methods, such as injection molding and roll-to-roll printing, for commercial viability compared to traditional pigment-based coloring.

Roll-to-roll printing is an emerging technology in the context of manufacturing micro- and nano-scale patterns and has been attracting interest because of its inherent advantages of low cost, high throughput and large area patterning [21, 22, 23, 24, 25, 26]. In recent years, a number of commercial applications have emerged, particularly optical displays, functional coatings and multifunctional films based on micron-sized structures [27]. Recently thermal roll-to-roll nanoimprint lithography with 100 nm one-dimensional grooves has been demonstrated [23], however general adaptation from the micro-scale to the nano-scale has proven difficult due to viscoelastic recovery in relatively fast printing processes. For these reasons thermal and pressure control of the imprint media are crucial. Based on previous work [28, 29] we now demonstrate two-dimensional 115 nm surface plasmon resonance structures with a high edge quality suitable for plasmonic color applications on a relatively large area.

Even though the printing speed used here is modest (0.3 m/min), the continuous roll process inherently makes it possible to process e.g. 500 m of film without stopping. By optimizing printing parameters, higher manufacturing speeds may be achieved if the pressure can be increased correspondingly. The web width (currently 60 mm) is completely scalable and thereby the system holds mass-volume capability.

Consequently, we report on plasmon structural colors produced by pattern transfer from a silicon master original, via a nickel shim, to a polymer surface using roll-to-roll techniques and subsequent metalization. Our study provides an engineering method to define a physical surface pattern that will yield a desired structural color, quantified by reflectance measurements. The use

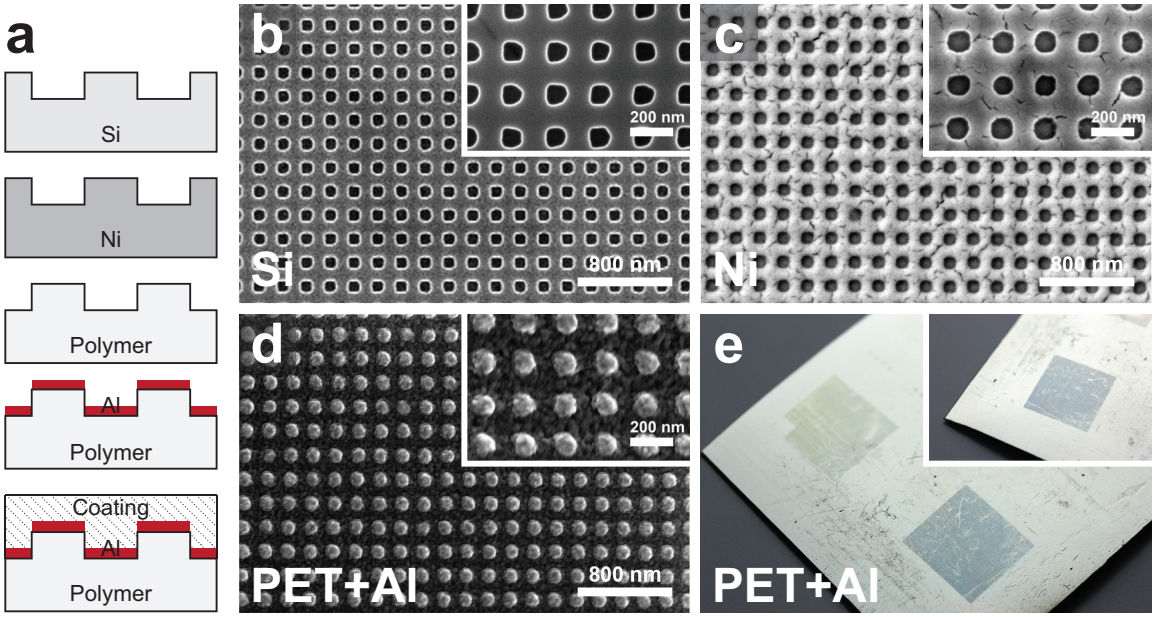

Figure 1: Fabrication process for 200 nm periodic structures from pattern definition to polymer metalized replica (blue area). a) Sketch. b) SEM images of Si master. c) SEM images of nickel master. d) SEM images of roll-to-roll polymer replication with aluminum on top. e) Photographs of the finished A-PET polymer surface without coating for 200 nm period (blue) and 300 nm period (green) areas of size 0.5 mm × 0.5 mm.

of roll-to-roll printing enables mass-volume production of plastic consumer surfaces with nano-scale based coloration for a wide range of applications.

2 FABRICATION

The fabrication process for making the plasmon colored samples is outlined in Fig. 1. First a silicon master was patterned by electron beam lithography and anisotropic dry etching. Subsequently, the silicon master was used in a double pattern inversion scheme to make a nickel shim with a thickness of 100 µm and a structure depth of 44 nm. The relatively thin nickel shim thickness was chosen due to the good bendabilty.

The replication process was carried out using a custom thermal roll-to-roll tool described in detail in Ref [21]. The nickel shim containing the structures for plasmonic colors was wrapped around a 66 mm diameter and 60 mm wide imprinting roll. Then a heated roll was pressed against a cold backing roll with a force of 600 N, resulting in a force between the rolls (NIP) of approximately 1000 N. The web materials tested included 100 um to 125 um thick polymethylmetcarylate (PMMA), polycarbonate (PC), amorphous polyethylene terephthalate (A-PET) and cellulose acetate (CA).

The temperature of the imprinting roll was adjusted to be above the film softening temperature, which is typically slightly below the glass transition temperature of the different materials. Roll-to-roll process printing temperatures are usually kept slightly below the film glass transition or the melting point temperature to avoid bending, wrinkling or other changes to the surface occurring at the glass transition temperature. Glass transition temperature for the used films, such as CA and PMMA, is 105 °C. For the A-Pet film, the glass transition temperature is 72 °C, but the melting temperature is 250 °C. A speed of 0.3 m/min was used, leading to an imprint time of roughly 0.3 s with a 3 mm contact length between the rolls. The contact length was varied by tuning the hardness of the backing roll. The best replication, with a disc diameter of 115 nm measured by SEM and a polymer structure depth of 40 nm measured by AFM, were obtained on A-PET at a printing temperature of 110 °C (± 2 °C).

After replication of the polymer samples, an aluminum metal layer was applied by electron beam evaporation in 2×10^{-6} mbar vacuum, see Fig. 1d. The deposition rate was 0.5 nm/s for a thickness of 16 nm measured by quartz crystal microbalance during deposition. Finally, samples were coated by approximately 50 µm of scratch-resistant commercial automotive lacquer. In terms of coating, the bulk part acts as a diffuser, mimicking the scattering properties of traditional paint, whereas the top surface of the coating creates a high-gloss visual appearance.

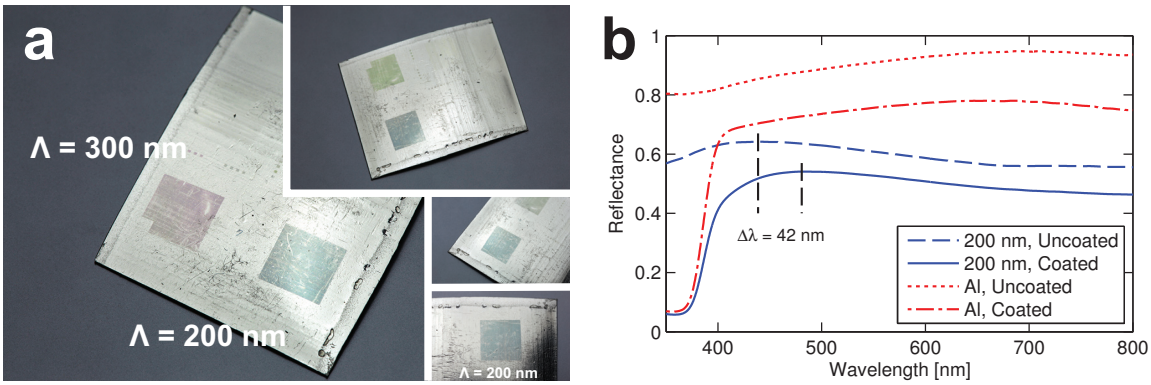

Figure 2: Sample after coating. a) Photographs with fixed light at different orientations. 200 nm period area has stable color response. b) Measured reflectance spectra by integrating sphere at 8 degrees incidence of 200 nm period area compared to non-structured aluminum surface. A red-shift is seen after coating.

3 RESULTS

Photographs taken under fixed light conditions of the sample after coating are shown in Fig. 2a. The sample scratches are due to the industrial grade film itself (CA from Clarifoil) and tear-and-wear mold degradation. The pattern with 200 nm period yields a distinct blue, angle-insensitive color-response, in agreement with simulation results (see supplemental material Figure S2 for Ref. [3]). Combined with the protective properties of the coating, our approach provides up-scalable production of durable structural colors.

In contrast to the blue 200 nm period pattern, the color-response of the 300 nm period pattern varies strongly with the orientation of the sample with respect to the light source and camera (see supplemental material). This dependence is well-described in literature [30, 3] and illustrates the requirement, due to the frequency-range of the human visible spectrum, for nano-scale patterns with periodicities in the order of 200 nm or smaller.

In Fig. 2b, measured reflection spectra by integrating sphere using a silicon specular reference can be seen for the 200 nm period pattern compared to the non-structured aluminum sample surface. A maximum in reflectance around a vacuum wavelength of 439 nm in the blue part of the spectrum is observed, as longer wavelengths are absorbed to a higher degree by the LSPR located in the red part of the spectrum. After coating, a red-shift of the maximum reflectance of approximately 42 nm can been be measured (the low ultra-violet reflectance is a property of the coating). This red-shift can also be directly observed by comparing photographs before and after coating (see Fig. 1e and 2a), where the blue color shifts to a blue-green color after coating. The red-shift of the maximum reflectance corresponds to a LSPR red-shift [3] and implies that the optical properties of the coating are important for the appearance.

4 CONCLUSION

In conclusion, we reported on the fabrication of plasmon color technology based on aluminum by LSPR using roll-to-roll printing on polymeric films. The use of the inherent mass-volume technique demonstrates a route for scalable production, which may lead to low-cost pattering and commercial uptake of plasmonic colors. Finally, nano-scale structural coloring provides new perspectives for recycling and sustainability of plastic products, as the colors are based on removable physical structures in the surface rather than traditional chemistry-based colorants.

ACKNOWLEDGMENTS

We acknowledge J. Scheel for photography. This work was supported by the European Commission via the FP7 MMP Integrated project Plast4Future (NMP2-SE-2012-314345).

REFERENCES

[1] Al-Salem, S. M., Lettieri, P., & Baeyens, J. (2009). Waste Management, 29(10), 2625-43. doi:10.1016/j.wasman.2009.06.004.

[2] Kumar, K., Duan, H., Hegde, R. S., Koh, S. C. W., Wei, J. N., & Yang, J. K. W. (2012). Nature Nanotechnology, 7(August), 557-561. doi:10.1038/nnano.2012.128.

[3] Clausen, J. S., Højlund-Nielsen, E., Christiansen, A. B., Yazdi, S., Grajower, M., Taha, H., & Mortensen, N. A. (2014). Nano Letters, 14(8), 4499-4504. doi:10.1021/nl5014986.

[4] Tan, S. J., Zhang, L., Zhu, D., Goh, X. M., Wang, Y. M., Kumar, K., ... Yang, J. K. W. (2014). Nano Letters, 14(7), 4023-4029. doi:10.1021/nl501460x.

[5] Si, G., Zhao, Y., Lv, J., Lu, M., Wang, F., Liu, H., ... Liu, Y. J. (2013). Nanoscale, 5(14), 6243-6248. doi:10.1039/c3nr01419c.
[6] Roberts, A. S., Pors, A., Albrektsen, O., & Bozhevolnyi, S. I. (2014). Nano Letters, 14(2), 783-787. doi:10.1021/nl404129n.
[7] Ramaswamy, A. L., & Kaste, P. (2005). Journal of Energetic Materials, 23(1), 1-25. doi:10.1080/07370650590920250.
[8] Jeurgens, L., Sloof, W., Tichelaar, F., & Mittemeijer, E. (2000). Physical Review B. doi:10.1103/PhysRevB.62.4707.
[9] Chan, G. H., Zhao, J., Schatz, G. C., & Duyne, R. P. Van. (2008). Journal of Physical Chemistry C, 112(36), 13958-13963. doi:10.1021/jp804088z.
[10] West, P. R., Ishii, S., Naik, G. V., Emani, N. K., Shalaev, V. M., & Boltasseva, a. (2010). Laser & Photonics Reviews, 4(6), 795-808. doi:10.1002/lpor.200900055.
[11] Knight, M. W., Liu, L., Wang, Y., Brown, L., Mukherjee, S., King, N. S., ... Halas, N. J. (2012). Nano Letters, 12(11), 6000-6004. doi:10.1021/nl303517v.
[12] Zhang, J., Ou, J.-Y., Papasimakis, N., Chen, Y., MacDonald, K. F., & Zheludev, N. I. (2011). Optics Express, 19(23), 23279-23285. doi:10.1364/OE.19.023279.
[13] Kulkarni, V., Prodan, E., & Nordlander, P. (2013). Nano Letters, 13(12), 5873-5879. doi:10.1021/nl402662e.
[14] Langhammer, C., Schwind, M., Kasemo, B., & Zoric, I. (2008). Localized surface plasmon resonances in aluminum nanodisks. Nano Letters, 8(5), 1461-1471. doi:10.1021/nl080453i.
[15] Chen, Q., & Cumming, D. R. S. (2010). Optics Express, 18(13), 14056-14062. doi:10.1364/OE.18.014056.
[16] Knight, M. W., King, N. S., Liu, L., Everitt, H. O., Nordlander, P., & Halas, N. J. (2014). ACS Nano, 8(1), 834-840. doi:10.1021/nn405495q.
[17] Zoric, I., Zch, M., Kasemo, B., & Langhammer, C. (2011). ACS Nano, 5(4), 2535-2546. doi:10.1021/nn102166t.
[18] Lochbihler, H. (2013). Optics Letters, 38(9), 1398-400. doi:10.1364/OL.38.001398.
[19] Olson, J., Manjavacas, A., Liu, L., Chang, W.-S., Foerster, B., King, N. S., ... Link, S. (2014). Proceedings of the National Academy of Sciences, 111(40), 14348-14353. doi:10.1073/pnas.1415970111.
[20] Prodan, E., Radloff, C., Halas, N. J., & Nordlander, P. (2003). Science, 302(5644), 419-422. doi:10.1126/science.1089171.
[21] Schleunitz, A., Spreu, C., Mäkelä, T., Haatainen, T., Klukowska, A., & Schift, H. (2011). Microelectronic Engineering, 88(8), 2113-2116. doi:10.1016/j.mee.2011.02.019.
[22] Mäkelä, T., Haatainen, T., & Ahopelto, J. (2011). Microelectronic Engineering, 88(8), 2045-2047. doi:10.1016/j.mee.2011.02.016.
[23] Kooy, N., Mohamed, K., Pin, L. T., & Guan, O. S. (2014). Nanoscale Research Letters, 9(1), 320. doi:10.1186/1556-276X-9-320.
[24] Peng, L., Deng, Y., Yi, P., & Lai, X. (2014). Journal of Micromechanics and Microengineering, 24(1), 013001. doi:10.1088/0960-1317/24/1/013001.
[25] Chang, C. Y., Yang, S. Y., & Sheh, J. L. (2006). Microsystem Technologies, 12(8), 754-759. doi:10.1007/s00542-006-0103-5.
[26] Yeo, L. P., Ng, S. H., Wang, Z., Wang, Z., & de Rooij, N. F. (2009). Microelectronic Engineering, 86(4-6), 933-936. doi:10.1016/j.mee.2008.12.021.
[27] Dumond, J. J., & Yee Low, H. (2012). Journal of Vacuum Science & Technology B: Microelectronics and Nanometer Structures. doi:10.1116/1.3661355.
[28] Mäkelä, T., Haatainen, T., & Ahopelto, J. (2011). Microelectronic Engineering 88, 2045-2047. doi:10.1016/j.mee.2011.02.016.
[29] Unno, N., Mkel, T., & Taniguchi, J. (2014). Journal of Vacuum Science & Technology B, Nanotechnology and Microelectronics, 32(6), 06FG03. doi:10.1116/1.4897132.
[30] Højlund-Nielsen, E., Weirich, J., Nørregaard, J., Garnaes, J., Asger Mortensen, N., & Kristensen, A. (2014). Journal of Nanophotonics, 8(1), 083988. doi:10.1117/1.JNP.8.083988.